Catena 195 (2020) 104810

Contents lists available at ScienceDirect

Catena

journal homepage: www.elsevier.com/locate/catena

Effect of the accuracy of topographic data on improving digital soil mapping predictions with limited soil data: An application to the Iranian loess plateau

Sedigheh Maleki[a], Farhad Khormali[a,*], Jahangir Mohammadi[b], Patrick Bogaert[c], Mohsen Bagheri Bodaghabadi[d]

[a] Department of Soil Science, Gorgan University of Agricultural Sciences and Natural Resources, Gorgan, Iran
[b] Department of Forest Science, Gorgan University of Agriculture Sciences and Natural Resources, Gorgan, Iran
[c] Earth & Life Institute, University Catholique de Louvain, Louvain-la-Neuve, Belgium
[d] Soil and Water Research Institute, Agricultural Research, Education and Extension Organization (AREEO), Karaj, Iran

ARTICLE INFO

Keywords:
Digital elevation model (DEM)
Limited data
Map accuracy
Random forest (RF)
Unmanned aerial vehicle (UAV)

ABSTRACT

The Iranian loess plateau is a unique area for its landscape and complex topography. There is however not any legacy soil data available for this region. Based on soil knowledge and previous evidences, it is known that various topographic attributes have considerable effects on soil development in such areas. To reach this goal, random forest (RF) models were used to relate a large set of environmental covariates and a total of 64 soil profiles in a part of the Iranian loess plateau.

The prediction of a soil map at four soil taxonomic levels was first carried out in an area of about 5390 ha. Geomorphology, elevation and aspect were the most important covariates that impact on the predictive performances of the soil map at each taxonomic level. The accuracy of the RF models was tested by 10-fold cross-validation and reported using the overall accuracy and Kappa index, which were equal to 76% and 0.56 at suborder level, 72% and 0.51 at great group level, 54% and 0.31 at subgroup level, and 40% and 0.23 at family level, respectively. Conversely, the results of uncertainty, as reported by the confusion index (CI), indicated that the uncertainty tends to increase towards lower taxonomic categories (i.e., from suborder to family level).

Having relied on the covariates importance, the impact of pixel size and accuracy of topographic attributes were assessed with the aim of improving the prediction at a comparison area of 210 ha. Two Digital Elevation Models (DEMs) were considered. The first one was derived from topographic lines initially drawn at 1:25,000 scale and a spatial resolution of 5 m (DEM A), while the second one was obtained at a 0.3 m spatial resolution (DEM B) using an Unmanned Aerial Vehicle (UAV). At the suborder level, the overall accuracy was 95% and 78% for the predicted maps with 0.3 × 0.3 m and 5 × 5 m pixel sizes, respectively. It is thus shown that the extracted DEM from a UAV technique can lead to an improved accuracy for the spatial prediction of soil maps at different taxonomic levels. Though this methodology could be used in other regions with limited soil data, its applicability and benefits could also depend on the specific topography variations, pedology knowledge and covariates at hand.

1. Introduction

The demand for soil maps is increasing over time as they are considered as a key element in many fields like, e.g., agricultural production (Keesstra et al., 2016), environmental pollution, climate change (Bouma, 1997) and precision agriculture (Stoorvogel et al., 2015). Soil maps are basic requirements in geoscience studies (Pahlavan Rad et al., 2014). They are however not at hand in many countries, especially at fine scales and at the national level (Zeraatpisheh et al., 2017). Considering the large extent of some countries, it is almost impossible to afford costly and time-consuming conventional soil survey methods for producing these maps (Dobos et al., 2001; Mulder et al., 2011) due to the large number of field observations they require (Stoorvogel et al., 2009). Soil spatial estimation methods, termed digital soil mapping (DSM, see McBratney et al., 2003), are thus regularly used as a substitute by soil scientists in order to account for available environmental covariates based on the *"scorpan"* model, with

* Corresponding author.
E-mail addresses: elymaleki@yahoo.com (S. Maleki), fkhormali@gau.ac.ir (F. Khormali), mohamadi.jahangir@gmail.com (J. Mohammadi), patrick.bogaert@uclouvain.be (P. Bogaert), m.baghery@areeo.ac.ir (M. Bagheri Bodaghabadi).

https://doi.org/10.1016/j.catena.2020.104810
Received 7 January 2020; Received in revised form 18 July 2020; Accepted 22 July 2020

$$S_c = f(s, c, o, r, p, a, n) + e \quad (1)$$

where S_c is a soil property or class and where the various inputs respectively relate to soil information, climate, organisms, relief, parent materials, age and spatial position, while e is an error term. Based on this idea, soil properties or classes have been predicted using a large set of linear and nonlinear techniques (e.g. geostatistics, Emadi and Baghernejad, 2014; fuzzy classification, Viloria et al., 2016; regression tree, Taghizadeh-Mehrjardi et al., 2014; multinomial logistic regression, Kempen et al., 2009; Abbaszadeh Afshar et al., 2018; Rasaei and Bogaert, 2019; random forest (RF), Pahlavan Rad et al., 2014; Sreenivas et al., 2016; Camera et al., 2017; Teng et al., 2018; Wang et al., 2018). The corresponding models are making use of environmental covariates that can be derived from digital elevation models (DEMs), geomorphology/geology maps and remotely sensed data (Mulder et al., 2011; Arrouays et al., 2014). In this study, RF has been used as it is considered as an accurate and computationally fast technique based on an ensemble of classification and regression trees (CART) that are aggregated to provide the final prediction (Breiman, 2001; Breiman and Cutler, 2004). RF models have several advantages for predicting soil types, as they are associated with high prediction performances with low biases, low variances and no overfitting issues (Zeraatpisheh et al., 2017). They can account both for continuous and categorical data (Grimm et al., 2008) and identify the relevant subset of variables to be used based on reiterative bootstrap sampling when creating each decision tree (Taghizadeh-Mehrjardi et al., 2016).

For arid and semiarid regions, topography is considered as the most important factor in the *scorpan* model (Jafari et al., 2013; Zeraatpisheh et al., 2017). It is thus expected that using DEMs for deriving relevant topographic attributes would be useful when it comes to predict soil types or soil properties (Bagheri Bodaghabadi et al., 2016), especially in areas characterized by important topographic variations. DEMs can be obtained from different methods, including field studies, existing topographic maps (Fabris and Pesci, 2005), or remote sensing from satellite or aerial photography (Höhle, 2009). New imaging techniques based on unmanned aerial vehicle (UAV) are also able to provide high-resolution information over relatively large areas (Hu et al., 2018). They can be used for mapping different aspects of the environment (Vega et al., 2015) and to reduce the burden of field-related activities (Hosseinalizadeh et al., 2019a). Numerous studies have highlighted the importance and accuracy of UAV techniques for land use mapping (Laliberte et al., 2010), microtopography and hydrological studies (Kung et al., 2011), landform map and terrain identification (Barneveld et al., 2013), detection of gully erosion (Hu et al., 2018) and spatial pattern modeling of gully headcuts (Hosseinalizadeh et al., 2019b). Nevertheless, they have rarely been used in soil mapping studies. Currently, there are only few studies (e.g. Cavazzi et al., 2013; Lacoste et al., 2014) that suggest the potential benefits of using higher resolution DEMs and their derivatives for improving soil map predictions when soil data are scarce, especially in arid and semiarid regions.

Despite the previously mentioned studies, DSM techniques are still rarely used in some parts of the world due to the lack of available soil data (Zhu et al., 2008; Stoorvogel et al., 2009; Zhao et al., 2020; Zeraatpisheh et al., 2020). This is typical when soil sampling is becoming difficult or impossible due to steep slopes, high elevations, rocky outcrops or lack of access paths. As emphasized in Table 1, numerous studies have been done using soil data sets involving more than 100 soil samples, but much less efforts have been devoted when considering smaller sample sizes.

As reported by Zeraatpisheh et al. (2020), soil data shortage is a common situation in many countries including Iran, where soil scientists are thus attempting to produce soil maps based on a limited set of field data. In parallel, little attention has been paid to the use of high-resolutions DEMs and their derivatives as an attempt to improve DSM in semiarid regions (Table 1). Accordingly, the present study aims to show how using high-precision environmental covariates can significantly help increase the quality of the predicted soil map. In our study, two scenarios are assessed: (i) soil classes are mapped at different taxonomic levels (i.e., suborder, great group, subgroup and family levels) and are predicted and validated with the same dataset using RF models by relying on the environmental covariates and a limited number of soil profiles in an area of 5390 ha; (ii) soil maps are predicted with two pixel sizes to investigate the effect of the spatial resolution of topographic data obtained from topographic lines at 1:25,000 scale (with 5 × 5 m raster resolution, denoted hereafter as DEM A) and from UAV technique (with 0.3 × 0.3 m raster resolution, denoted hereafter as DEM B) for improving DSM predictions at a 210 ha comparison area. The corresponding predicted soil maps are compared and the benefit of high-resolution covariates for improving predictions of soil mapping is discussed.

Overall, the methodology proposed here is believed to be innovative with respect to at least two aspects: (i) using a limited soil data set to map soil classes at different taxonomic levels, and (ii) to the best of our knowledge, there is no previous study at such a high (i.e. 0.3 × 0.3 m) spatial resolution that relies on UAV techniques for DSM. This study could hopefully be useful in similar situations in other regions, by highlighting how high-resolution topographic attributes can at least partially compensate for the lack of soil data when it comes to predict soil maps.

2. Materials and methods

The workflow used in this study is summarized in Fig. 1 and includes four phases, i.e., (i) selection of the study areas through two mentioned scenarios; (ii) data preparation (field investigation, environmental covariates, aerial photos and DEMs, soil sampling and laboratory soil analysis), (iii) soil maps prediction using RF at different taxonomic levels, and (iv) final validation of these maps.

2.1. Description of the study area

The study area is a part of the Iranian loess plateau, located in Golestan province (Fig. 2), where no soil mapping studies were previously conducted. It covers an area of 5390 ha (55°13′ 26″–55°09′ 36″ E and 37°36′ 37″–37°41′ 41″ N) (Fig. 2c), with 350 mm mean annual precipitation and 17 °C mean temperature. The main land uses are crops and rangeland. The area has experienced intensive human activities, especially in flat parts for wheat production. The soil moisture and temperature regimes are dry Xeric and Thermic, respectively (Soil Survey Staff, 2014). The parent material is varying from North to South and is composed of marl, marl dominant with shale and loess, limestone, clay deposits and reddish-brown lower Pleistocene loess (LPL), loess deposit and reworked loess. The loess deposits preserve valuable information on climate change and landscape development during the Quaternary (Khormali and Kehl, 2011). Due to a complex topography and the lack of appropriate access paths, little information is available on soil development and geomorphology of the region. It is however known that in the semiarid climate of this loess plateau, aspect plays an important role on soil development through the preservation of moisture and dense vegetation for north-facing slopes, unlike south-facing ones (Maleki et al., 2018). According to the role of topography on soil development, a part of the study area, referred hereafter as the comparison area (Fig. 2c), was selected in order to compare and evaluate the effect of spatial resolution of topographic attributes for soil mapping. This comparison area is about 210 ha (55°08′ 55″–55°09′ 47″ E and 37°37′ 10″–37°37′ 49″ N) and is characterized by a loess parent material.

2.2. DEM and aerial images obtained from UAV

An UAV technique was used to obtain aerial images and to build a DEM at a 0.3 m spatial resolution over the comparison area. The UAV

Table 1
Summary of representative DSM publications predicting soil classes or properties.

References	Region	Spatial extent	Soil attribute	Number of observations	Spatial resolution of DEM
Zhu et al. (2008)	Heilongjiang, China	6000 ha	Class	45	10 m
Brungard (2009)	Southwestern Utah, USA	30,000 ha	Class	300	10 m
Stoorvogel et al. (2009)	Senegalese Peanut Basin	103,000 ha	SOC	40	30 m
Jafari et al. (2013)	Zarand, Iran	90,000 ha	Class	126	30 m
Pahlavan Rad et al. (2014)	Golestan, Iran	85,000 ha	Class	99	30 m
Zeraatpisheh et al. (2017)	Borujen, Iran	86,000 ha	Class	100, 80, 60	30 m
Yiming et al. (2017)	Anhui, China	1.34×10^7 ha	SOC	282	90 m
Abbaszadeh Afshar et al. (2018)	Bam, Iran	100,000 ha	Class	126	30 m
Mirakzehi et al. (2018)	Sistan, Iran	60,000 ha	Class	108	30 m
Rasaei and Bogaert (2019)	Iran	1.05×10^6 ha	Class	390	90 m
Silva et al. (2019)	Posses watershed, Brazil	1200 ha	Class	74	20 m

SOC: Soil organic carbon

was DJI Phantom-2 quadcopter (DJI, 2016) equipped with a Gopro Hero3 + digital camera capable of recording 12 MP images (Fig. 3a). Before flying, ground control points (GCP) were located using a Trimble R3 differential GPS (DGPS). The longest flight time was about 30 min. A total of 212 RGB (Red-Green-Blue) images were obtained in jpeg format under calm weather conditions (e.g. sunny, with no clouds and rainfall). Images were quality controlled, i.e. images taken during take-off and landing or in general images reducing the quality of the processing or increasing the processing time were discarded (Liu et al., 2018). The Pix4Dmapper software version 2.0.100 (see https://pix4d.com) was used to extract orthophotos and the DEMs over the comparison area.

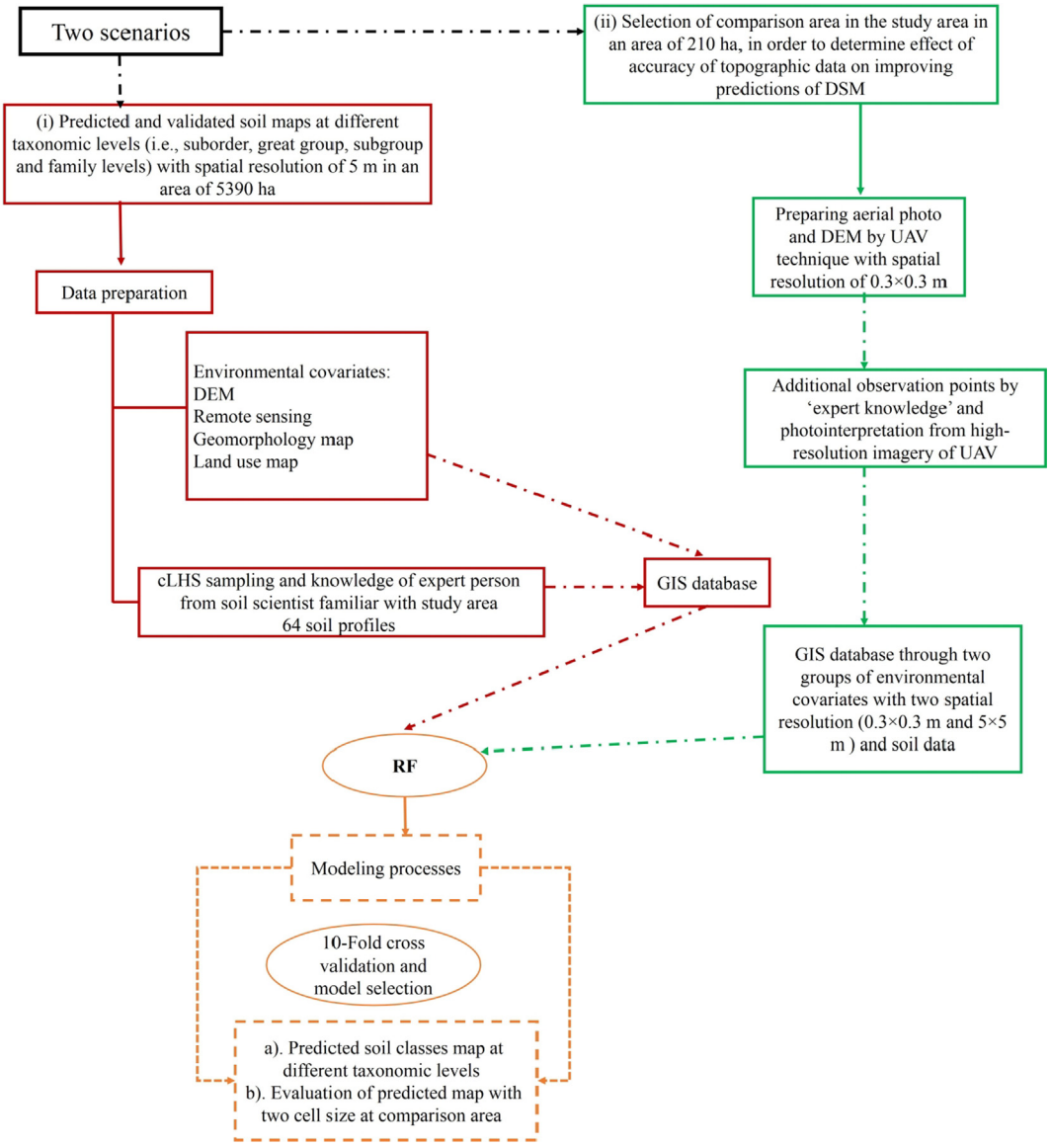

Fig. 1. Workflow of the methodology used in this paper.

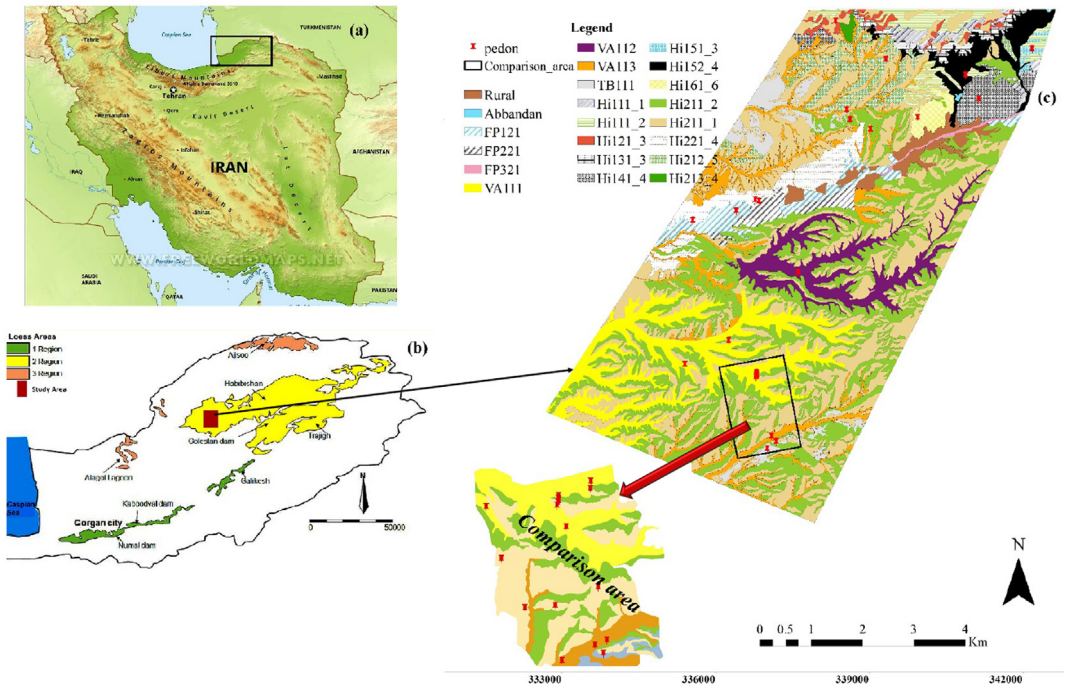

Fig. 2. (a) Golestan province in Iran (b) loess areas (Feiznia et al., 2005) and location of the study area (red rectangle) in the Iranian loess plateau (c) the geomorphic surfaces map of the study area (Maleki et al., 2018). Codes in geomorphic surface map: FP121: Meanders belt, erosional surface, cultivated, FP221: Erosional or depositional terraces, cultivated, FP321: Gully, uncultivated, VA111: Moderately flat, cultivated, VA112: Moderately flat with sinkhole and gully erosion in some part, cultivated, VA113: Narrow valley with sinkhole and gully erosion in some part, cultivated, TB111: A relatively flat- topped area with steep side slopes, cultivated, Hi111_1: Very steep complex slopes, south aspect, low density rangeland, Hi111_2: very steep complex slopes north aspect, dense rangeland, Hi121_3: Complex aspect, no rangeland, Hi131_3: Steep complex aspect, no rangeland, Hi141_4: Steep complex aspect, low density rangeland, Hi151_3: Steep complex aspect, no rangeland, Hi152_4: Complex aspect, low density rangeland, Hi161_6: Complex aspect, moderate density rangeland, Hi211_2: Moderately complex slope, north aspect, dense rangeland, Hi211_1: Moderately complex slope, South aspect, low density rangeland, Hi212_5: Very steep complex slopes, north aspect, moderate dense rangeland, Hi213_4: Very steep complex slopes, complex aspect, low density rangeland, Hi221_4: Steep complex slopes, complex aspect, low density rangeland.

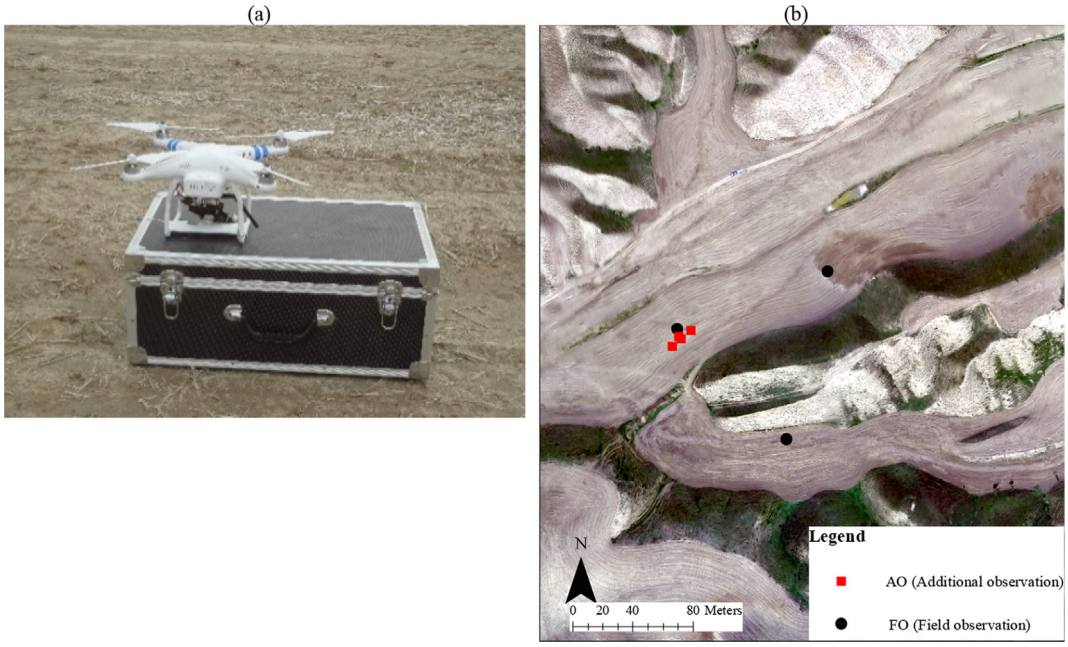

Fig. 3. (a) the DJI Phantom-2 UAV that was used for image acquisition in this study (Photo taken by first author), (b) one of the UAV image over the comparison area at 0.3 m spatial resolution, along with the locations the additional observations and field observations on the UAV image.

2.3. Environmental covariates

Various environmental covariates including geomorphology map, topographic attributes and remotely sensed index were used in this study, as illustrated in Table 2. The soil adjusted vegetation index (SAVI, Huete, 1988) was calculated from a Landsat 8 image acquired on February 25, 2014 (U.S. Geology survey, 2014; http://glovis.usgs.gov) and processed in the ENVI 4.4 software. Topographic attributes were

Table 2
Environmental covariates used as predictors in scenarios 1 and 2.

Environmental data	Soil forming factor	Parameter used in scenario1	Parameter used in scenario 2	Symbol	Variable type	Reference
Topographic attributes	Topography	Elevation	*	ELV	Quantitative	Wilson and Gallant (2000)
		Slope	*	Slope		
		Aspect	*	ASP		
		Curvature	–	Curv		
		Profile curvature	–	Profcurv		
		Plan curvature	–	Plancurv		
		Convergence	–	Converg		
		Classcurvature	–	Classcurv		
		Relative slope	*	Reltslp		
		Flow accumulation	–	Flowacc		
		Stream power index	*	LS		
		Topographic wetness index	*	TWI		
		Valley depth	*	valley		Gallant and Dowling (2003)
		Multi-resolution valley bottom flatness index	*	Mrv		
		Multi-resolution of ridge top flatness index	*	Mrr		
		Topographic position index	*	TPI		Weiss (2001)
Remote sensing attributes	Vegetation	Soil adjusted vegetation index	*	SAVI		Huete (1988)
Landuse map		Landuse	*	landuse	Categorical	–
Geomorphology map	Parent material, topograpy, soil	Geomorphology units	*	landform	Categorical	Toomanian et al. (2006)

The *symbol indicates the environmental covariates which were used for the comparison area with two spatial resolutions of 0.3 m and 5 m (scenario 2).

derived from DEMs in the SAGA GIS software (Olaya, 2004). It should be noted that the 5 m DEM over the study area was acquired from topographic lines initially drawn at the 1:25,000 scale generated by the National Cartographic Center of Iran. The 10 m resolution DEM was corrected and resampled at 5 m resolution according to our need (see Hengl, 2006) using 600 elevation points obtained by theodolites. Previous research by Kramm et al. (2017) in the Iranian loess plateau showed that 5 m DEM achieved accuracies greater than 70% to generate classification of geomorphic map and topographic attributes, while SRTM, ASTER GDEM and 10 m DEMs were not able to generate accurate classification results. Therefore, there was a need for a grid resolution that optimally reflects the variability of the elevation surface (Hengl, 2006) and terrain complexity in our study area. To evaluate the accuracy of the 5 m resolution DEM, 175 ground-truth points of Trimble R3 DGPS were obtained during the field campaign. For each point, the altitudes of the datasets were compared to the DGPS heights.

In parallel, the 0.3 m DEM (DEM B) obtained from UAV over the comparison area were also used to extract topographic attributes in order to investigate the effect of the spatial resolution of topographic data on DSM. Geomorphic units were defined using aerial photo interpretation (Zinck, 1989; Toomanian et al., 2006) from Google Earth satellite imagery (Quickbird) and from UAV orthophotos in the study and comparison areas, respectively. Pedologic and geomorphologic knowledge (i.e., the relationship between soils and soil forming factors) was used to delineate geomorphic units. Twenty geomorphic units were identified in the study area (Fig. 2c). More details regarding geomorphic units can be found in Maleki et al. (2018). It should be noted that geomorphic units prepared from UAV orthophotos were used for two DSM frameworks in scenario 2. The environmental covariates were used as predictors in these scenarios, as shown in Table 2.

2.4. Sampling scheme and profile description

The conditioned Latin Hypercube sampling (cLHS; Minasny and McBratney, 2006) was used for all covariates mentioned in Table 2 at a 5 m spatial resolution based on a Matlab script (MathWorks, 2009). For semi-detailed soil survey studies, one observation per 100 ha is usually recommended (Rossiter, 2000). Therefore, 54 samples were considered for the study area of 5390 ha. Due to lack of maps and soil information over this study area, expert person knowledge was also used for checking and sampling in the field. Based on an initial set of 90 potential locations that were generated from cLHS, few profiles were first selected and dug in the study area based on the expert knowledge of field scientists. Kempen et al. (2009) emphasized that expert pedology knowledge is indeed a key factor in building the model structure to ensure correct pedological and statistical outputs, while Arrouays et al. (2020) warned against the risks of blindly replacing pedological knowledge with automated and machine-learning techniques. A total of 64 profiles were finally selected and dug (Fig. 2c) by combining at best cLHS and expert knowledge. All profiles were described, sampled, analysed, and classified up to the family level of the US Soil Taxonomy (Soil Survey Staff, 2014).

2.5. Random forest models

A RF model is the result of an ensemble of randomized decision trees that are used in order to improve the prediction accuracy (Breiman, 2001). Each decision tree is obtained using bootstrap sampling from the training data, using about 2/3 of the training data. Similarly, a subset of the environmental covariates used to classify the nodes is also chosen randomly for each tree. Two user-defined parameters are important in RF: the number *mtry* of environmental covariates used in each random subset and the number *ntree* of trees used in the forest. Both parameters were optimized by iterating over *mtry* values ranging from 1 to the total number of covariates (19 in our study) while *ntree* values were ranging from 100 to 10,000 by increments of 100 (Zhi et al., 2017). Additionally, *mtry* can also be selected based on the calculation of the square root of total number of independent variables (Mohammadi et al., 2017).

For our study, the importance of each covariate in the RF algorithm was assessed using two methods, which are the mean decrease in accuracy and the mean decrease in Gini (Myles et al., 2004) based on the so-called out-of-bag error (Peters et al., 2007, Taghizadeh-Mehrjardi et al., 2016, Zhi et al., 2017), where

$$\text{OOB error} = \frac{1}{N}\sum_{i=1}^{N} I\left[Y_{OOB}(X_i) \neq Y_i\right] \quad (2)$$

with $I\left[Y_{OOB}(X_i) \neq Y_i\right]$ an indicator function equal to 0 when the predicted and actual classes are the same and equal to 1 otherwise. For the mean decrease in accuracy method, the true values of the variables are replaced by values that are randomly generated for each tree and the effect of this substitution on the prediction accuracy is computed. If this substitution has no effect on the OOB error, the corresponding variable is of low importance (Breiman and Cutler, 2004). The mean decrease in Gini is measuring covariates importance by permuting the values of each environmental covariate in OOB samples, so that environmental covariates associated with the highest OOB error increase are the most important ones (Breiman, 2001).

Modeling of Soil Taxonomy at the suborder, great group, subgroup and family levels and assessing covariates importance was done using the "randomForest", "rpart", and "caret" packages (Liaw and Wiener, 2002) in R version 3.4.3 (R Development Core Team, 2017) and RStudio version 1.1.383 (RStudio, 2009–2017). The RF algorithm was run too for the comparison area (scenario 2) with two spatial resolutions (5 × 5 m and 0.3 × 0.3 m) for the environmental covariates and using 19 soil profiles. However, as the number of soil profiles in the comparison area is low, this is sufficient for a detailed soil survey study as previously described in Section 2.4. While RF algorithms used in DSM have shown acceptable performances (Camera et al., 2017; Silva et al., 2019), concerns about the occurrence of unbalanced soil classes are still raised on different landscapes. These soil classes can have significant effects on the process of model fitting, model selection, and output accuracies (Silva et al., 2019). Hence, additional observations (AO) were selected, since increasing the number of field sampling points is time-consuming and economically infeasible. The methodology is explained in Silva et al. (2019).

As the dominant soil mapping class was the Haploxerepts (representing 10 of the soil samples at the comparison area), this leads to highly imbalanced frequencies between classes. To overcome this issue, AO were added for the less common soil classes (i.e. Calcixerepts and Xerorthents) based on expert knowledge and photointerpretation from high-resolution UAV imagery (Fig. 3b). The AO were increased until the model training was well fitted according to the Kappa and overall accuracy. The best models with the optimum dataset size were selected after 100 repetitions of a 10-fold cross-validation procedure. As a result, DSM at the comparison area was conducted using the environmental covariates and 25 pedons (i.e. using six AO and the initial 19 field observations). Although the soil data was limited in this study, one of our goals was to precisely evaluate the performance of RF models based on limited soil observations but using high-resolution covariates, so that the findings could be extended to future DSM studies in regions with limited soil database. As noted by Khaledian and Miller (2019), RF is not sensitive to the number of observation points and thus appears as a sound choice in our context.

2.6. Model evaluation

In this study, 10-fold cross-validation was used to test and evaluate the results of RF models. Taghizadeh-Mehrjardi et al. (2016) explained that this method is reliable and leads to unbiased results for small datasets. The overall accuracy (Brus et al., 2011) and Kappa index (Marchetti et al., 2011) are two error criteria that are widely used in DSM approaches for building the training and test data sets (Brungard et al., 2015) and for selecting the best model. Overall accuracy (OA) corresponds to the total classification accuracy (Brus et al., 2011), with

$$OA = \frac{\sum_{i=1}^{n} N_{ii}}{N} \quad (3)$$

where N_{ii} are the diagonal counts in the error matrix, N is the total number of counts and n is the number of soil classes. The Kappa index (K) is correcting this OA by accounting for the fact that part of the agreement between predicted and true classes is due to chance (Maleki et al., 2018; Abbaszadeh Afshar et al., 2018), so that

$$K = \frac{OA - CA}{1 - CA} \quad (4)$$

where CA is this chance agreement.

The producer's accuracy (PA) is the accuracy from the point of view of the soil map maker (the producer), i.e. the chance that the *j*th soil class is correctly classified when this soil class is the correct one (as measured by N_{+j}, the sum of the counts in the *j*th column of the error matrix), with

$$PA_j = \frac{N_{ii}}{N_{+j}} \quad (5)$$

The user's accuracy (UA) is the accuracy from the point of view of the map user, i.e. the chance that the *j*th soil class is correctly classified when this soil class is the predicted one (as measured by N_{i+}, the sum of the counts in the *i*th line of the error matrix), with

$$UA_i = \frac{N_{ii}}{N_{i+}} \quad (6)$$

For more details about PA and UA for soil maps, see e.g. Bagheri Bodaghabadi et al. (2016).

2.7. Assessment of prediction uncertainty

In DSM, the resulting predictions are always slightly erroneous, and as a result, predictions are accompanied by uncertainty. On the other hand, uncertainty is the result of a lack of confidence in reality while the overall accuracy/ error represents the differences between observed and predicted values of soil classes (Minasny and Bishop, 2008).

The Confusion Index (CI; Brungard et al., 2015; Esfandiarpour-Boroujeni, et al., 2020) was used to report the prediction uncertainty at each taxonomic level. In this method, the probable presence of each soil class per pixel is calculated and CI is calculated as

$$CI = \left|1 - (\lambda_{\max} - \lambda_{\max-1})\right| \quad (7)$$

where $\lambda_{\max}$ is the maximum probability per pixel and $\lambda_{(\max-1)}$ is the second highest probability per pixel. The CI values are thus in the [0,1] interval, with higher values corresponding to higher uncertainties (Esfandiarpour-Boroujeni, et al., 2020).

3. Results and discussion

3.1. Soil descriptions

The description of the various soil taxonomic levels for the 64 sampled soil profiles is given in Table 3. Inceptisols and Entisols were the main observed soil orders (60 profiles), with few Alfisols (4 profiles). It should be mentioned that Alfisols are relict paleosols developed in reddish brown lower Pleistocene loess (LPL) with intensive pedogenesis including secondary carbonate and gypsum, Fe-Mn coating, and clay skins from more humid past climates in this area (Taheri et al., 2016). In general, Inceptisols were mostly located in flat and north-facing slopes while Entisols were concentrated in south-facing steep slopes, thus confirming that soils in the study area are severely affected by topography. The most observed soil taxonomic classes at the subgroup and family levels were also related to Inceptisols comprising 48.4% of the study area (Table 3).

The lower soil diversity at the suborder and great group levels is attributed mainly to the semiarid climate of the study area. The higher soil diversity at the family level could be related to differences in parent material, erosion, transportation and sedimentation of materials.

Table 3
Observed soil taxonomic classes and number of observations per class.

Order	N	Suborder	n	Great Group	n	Subgroup	n	Family	n
Inceptisols	31	Xerepts	31	Calcixerepts	4	Typic Calcixerepts	4	Fine-loamy, mixed, active, thermic, Typic Calcixerepts	4
				Haploxerepts	27	Gypsic Haploxerepts	7	Coarse-loamy, mixed, active, thermic, Gypsic Haploxerepts	4
								Fine-loamy, mixed, active, thermic, Gypsic Haploxerepts	3
						Typic Haploxerepts	20	Fine-loamy, mixed, active, thermic, Typic Haploxerepts	16
								Coarse- Loamy, mixed, active thermic, Typic Haploxerepts	4
Entisols	29	orthents	29	Xerorthents	29	Lithic Xerorthents	3	Fine-loamy, mixed, active, thermic, Lithic Xerorthents	3
						Typic Xerorthents	26	Fine-loamy, mixed, active, thermic, Typic Xerorthents	13
								Coarse-loamy, mixed, active, thermic, Typic Xerorthents	10
								Fine, mixed, active, thermic, Typic Xerorthents	3
Alfisols	4	Xeralfs	4	Haploxeralfs	4	Calcic Haploxeralfs	4	Fine, mixed, active, thermic, Calcic Haploxeralfs	4

Table 4
Results for Kappa index, overall accuracy, and confusion idex (CI) at different soil taxonomic levels.

Taxonomic level	Frequency	Overall accuracy	Kappa index	CI
Suborder	3	76	0.56	0.06–0.64
Great Group	4	72	0.51	0.03–0.80
Subgroup	6	54	0.31	0.04–0.96
Family	10	40	0.23	0–1

3.2. Model performance

3.2.1. Model accuracy and uncertainty

High values of Kappa index and overall accuracy (above 70%) were obtained at the suborder and great group levels (Table 4). Conversely, the lowest Kappa index and overall accuracy were obtained at the family level (Table 4). These results agree with those of Pahlavan Rad et al. (2014) who used 99 soil profiles and found overall accuracy and Kappa index values equal to 51.9% and 0.31, respectively at great group level, and the lowest values at series level. Esfandiarpour-Boroujeni et al. (2020) reported overall accuracy of 86%, 73%, 60%, and 30% at suborder, great group, subgroup, and family levels, respectively, using 120 soil profiles in the Shahrekord plain, Central Iran. This agrees too with results of Zeraatpisheh et al. (2017) and Mirakzehi et al. (2018) who observed decreasing values of Kappa index and overall accuracy at the lower taxonomic levels. Our results, therefore agree well with those of the previous studies, with reasonably better predicted soil maps at different taxonomic levels based on limited data. The main reason could be attributed to the use of high precision covariates, especially geomorphology map and some topographic derivatives, which will be discussed in detail in Sections 3.2.2 and 3.3.

A tentative conclusion is that reducing field observations and preparing soil maps at higher taxonomic levels can be an alternative when financial issues and the lack of legacy soil data are limiting factors, which will however be at the price of a lower accuracy. According to Zeraatpisheh et al. (2017), reducing the sampling density from 100 to 80 (or to 60) observations reduces the preparing cost of the map by 20% (or by 40%), although Kappa index and map purity do not decrease at the same rate. They showed that Kappa index slightly decreased from 0.46 to 0.33 when sampling density reduced from 100 to 60 points at the order level while the map purity was still equal to 0.6. Their results also indicate that Kappa index and map purity showed little difference at different taxonomic levels (order, suborder, great group, and subgroup) with different sample densities. In this regard, Zhu et al. (2008) predicted a soil map in China at the subgroup level (overall accuracy of 76%) with limited soil data (45 observations) by using high-resolution auxiliary information, thus significantly reducing the sampling costs and time.

It should also be noted that, from suborder to family levels, the range of values for CI is increasing (Table 4), while conversely overall accuracy is decreasing. This can be related to a higher number of soil classes and thus a lower number of samples in each of these classes. As shown in Table 4, the number of soil classes increases from 3 at the suborder level to 10 at family level. Clearly, the number of soil classes play an important role in the quality of the results. Similar results are reported by Esfandiarpour-Boroujeni et al. (2020). At suborder and great group levels, overall accuracy is quite similar, with a lower CI range at the suborder level than at the great order level. The accuracy of the predicted map is not the sole factor to explain the quality of the map, but its uncertainty is important as well. Some studies (e.g., Lagacherie et al., 2019; Machado et al., 2019; Esfandiarpour-Boroujeni et al., 2020) have interpreted the importance of uncertainty assessment in predicting soil map.

The results of UA and PA for predicted classes at different taxonomy levels generally confirm that classes with higher number of observations have higher UA and PA. As seen in Table 5 and Fig. 4, the highest number of soil profiles at subgroup level is observed for the Typic Haploxerepts and Typic Xerorthents classes, which have the highest (above 60%) UA values. In general, soil classes with higher sampling frequencies have higher UA's and PA's. Results reported by Kempen et al. (2009), Brungard (2009), Pahlavan Rad et al. (2014), Mosleh et al. (2016), and Rasaei and Bogaert (2019) are in line with those presented here.

The class of Fine, mixed, active, thermic, Typic Xerorthents at family level (Table 5) had a UA of 66.7% and PA of 100% in spite of its low sampling frequency, while the class of Fine-loamy, mixed, active, thermic, Gypsic Haploxerepts (with the same observations) exhibits a UA and PA equal to 0%. However, there is a big difference in the frequencies and land areas of these two classes at the subgroup level (Gypsic Haploxerepts and Typic Xerorthents), with a distinct UA difference (0% and 92.3%, respectively). This is explained by the fact that the strong relations of soil classes to some covariates could result in a lower error even if their sampling frequency is lower than other classes (Pahlavan Rad et al., 2014). Mosleh et al. (2016) also considered the accuracy as being influenced by factors like soil variability, number of soil samples and the ability of environmental covariates to explain soil variations.

3.2.2. Covariate importance

As identified from the mean decrease in accuracy and the mean decrease in Gini, the most important covariates are geomorphology, elevation and aspect at suborder, great group and subgroup levels. At family level, geomorphology, elevation, valley depth and TPI are the most important ones (Fig. 5). The role of geomorphological processes is thus confirmed at these four taxonomic levels. These results also agree with those of Behrens et al. (2005), Jafari et al. (2013), Taghizadeh-Mehrjardi et al. (2014), and Zeraatpisheh et al. (2017) who observed the positive impact of using geomorphology maps when predicting soil classes. For arid and semiarid regions, it is usual that the variability of soil properties and classes are affected by parent material and topographic position, which are features that are well captured by a geomorphology map. The lower impact of aspect at soil family level can be

Table 5
Results for user's accuracy (UA) and producer's accuracy (PA) at suborder, great group, subgroup, and family levels.

Level	Class	Frequency	Area (ha)	UA (%)	PA (%)
Suborder	Xerepts	31	2777	80.6	83.3
	Orthents	29	2168	86.2	73.52
	Xeralfs	4	79	0	0
Great group	Haploxerepts	27	2674	81.5	75.9
	Xerorthents	29	2194	89.6	74.2
	Calcixerepts	4	24	0	0
	Haploxeralfs	4	132	0	0
Subgroup	Gypsic Haploxerepts	7	309	0	0
	Typic Haploxerepts	20	2280	65.0	50.0
	Typic Xerorthents	26	2246	92.3	72.7
	Typic Calcixerepts	4	45	0	0
	Calcic Haploxeralfs	4	140	0	0
	Lithic Xerorthents	3	4	0	0
Family	Coarse-loamy, mixed, active, thermic, Gypsic Haploxerepts	4	384	0	0
	Fine-loamy, mixed, active, thermic, Typic Haploxerepts	16	2004	75.0	41.3
	Fine-loamy, mixed, active, thermic, Gypsic Haploxerepts	3	25	0	0
	Fine-loamy, mixed, active, thermic, Typic Xerorthent	13	1263	30.7	28.5
	Coarse-loamy, mixed, active, thermic, Typic Xerorthents	10	829	50.0	41.6
	Coarse- Loamy, mixed, active thermic, Typic Haploxerepts	4	152	25.0	100
	Fine-loamy, mixed, active, thermic, Typic Calcixerepts	4	102	0	0
	Fine, mixed, active, thermic, Calcic Haploxeralfs	4	160	0	0
	Fine-loamy, mixed, active, thermic, Lithic Xerorthents	3	15	0	0
	Fine, mixed, active, thermic, Typic Xerorthents	3	91	66.7	100

explained by the influence of elevation, TPI, valley depth and land use on sediment transfer and erosion. The results of Brungard et al. (2015) showed that the most accurate spatial predictions were generally in agreement with the expected soil-landscapes relationships and topographic derivatives.

3.3. Effect of spatial resolution of topographic attributes through scenario 2 in comparison area

For the comparison area, the soil classes were predicted using topographic attributes and geomorphology map as obtained from the UAV technique at a 0.3 m spatial resolution and from the topographic attributes at a 5 m spatial resolution. Due to the lack of enough soil observations for some classes, soil modeling was not performed at family level since RF modeling requires more than three observations per class to meaningfully predict the probability of the class (Brungard et al., 2015).

3.3.1. Model accuracy and uncertainty

The results for the overall accuracy and Kappa index are presented in Fig. 6 at the 0.3 m and 5 m resolutions. The same training data were used for both pixel sizes, so that the effect of the spatial resolution on the model accuracy can be compared. Using the 0.3 m resolution for the environmental covariates yields better performance at three taxonomic levels compared to the 5 m DEM, with Kappa index and overall accuracy equal to 95% and 0.90 at suborder level, and 83% and 0.75 at great group and subgroup levels (Fig. 6). These results also confirm that using DEM B increases the accuracy of the predicted soil maps, with the overall accuracy and Kappa index increase by about 17% and 20%, respectively at the suborder, great group and subgroup levels. Additionally, the results of CI indicate that the predicted map at 0.3 m resolution was more reliable than at 5 m resolution at three taxonomic levels (Table 6). This suggests that accurate high-resolution environmental covariates have a beneficial effect on the accuracy and uncertainty of the class prediction. In parallel, the UA at different taxonomic levels ranges from 75% to 93% and from 45.4% to 90% for the 0.3 m and 5 m spatial resolutions, respectively (Table 6). The lowest performances of UA and PA at 0.3 m resolution are observed for soil classes with the lowest sampling frequencies (i.e. Calcixerepts and Typic Calcixerepts). It is thus expected that UA could be reduced by increasing the number of observations in these classes. The results of Table 6 also show that using DEM B increases the UA of the predicted soil classes (i.e. Haploxerepts and Typic Haploxerepts classes) by about 37% compared to DEM A. Only the five Haploxerepts and Typic Haploxerepts classes at the great group and subgroup levels (out of the 11 identified frequencies) were correctly predicted by the 5 m resolution (see UA results in Table 6; confusion matrix not shown here).

From Table 6, the maximum predicted areas are associated with Xerepts, Haploxerepts, and Typic Haploxerepts at both spatial resolutions, though there are differences in these predicted areas depending on the resolution, as illustrated too in Fig. 7a and b. This difference in predicted areas can be important for some classes depending on the availability of soil samples. Typic Calcixerepts for instance, have a predicted area that doubles when predicted at a 5 m resolution, and it can be seen from Fig. 7b that this soil subgroup is predicted on valley landform where soil samples are at hand.

An interesting point from Fig. 7c is that the soil map obtained from UAV is consistent with the corresponding orthophoto. Mukherjee et al. (2013) also compared some DEM-derived topographic attributes like slope and drainage network density as obtained from ASTER and SRTM. They stated that the accuracy of the topographic derivatives was directly related to the DEM used. Likewise, Lacoste et al. (2014) predicted SOC map using topographic attributes derived from a 2 m light detection and ranging DEM (LiDAR DEM) combined with 70 soil samples over a 10 km^2 area. They extracted the topographic derivatives from the 2 m DEM resampled at 5, 10 and 20 m. They concluded that terrain attributes at the 5 m spatial resolution yield better performance for all soil layers.

In combination with field checking, UAV images are valuable inputs for the proper identification of the relationship between soil classes and environmental covariates. However, there are two potential issues associated with the use of high-resolution DEMs: (i) using smaller pixels leads to topographic attributes that may include very local spatial features that are irrelevant when related to soil classes, thus increasing the noise in the covariates and negatively impacting the quality of the predicted maps, and (ii) using smaller pixels requires larger storage capacity and induces longer processing time. In our study area, soil classes in hillslopes were better predicted using the high-resolution DEM (Fig. 7b), which is also consistent with Pain (2005) and Cavazzi et al. (2013) who suggested that high-resolution DEMs are needed for

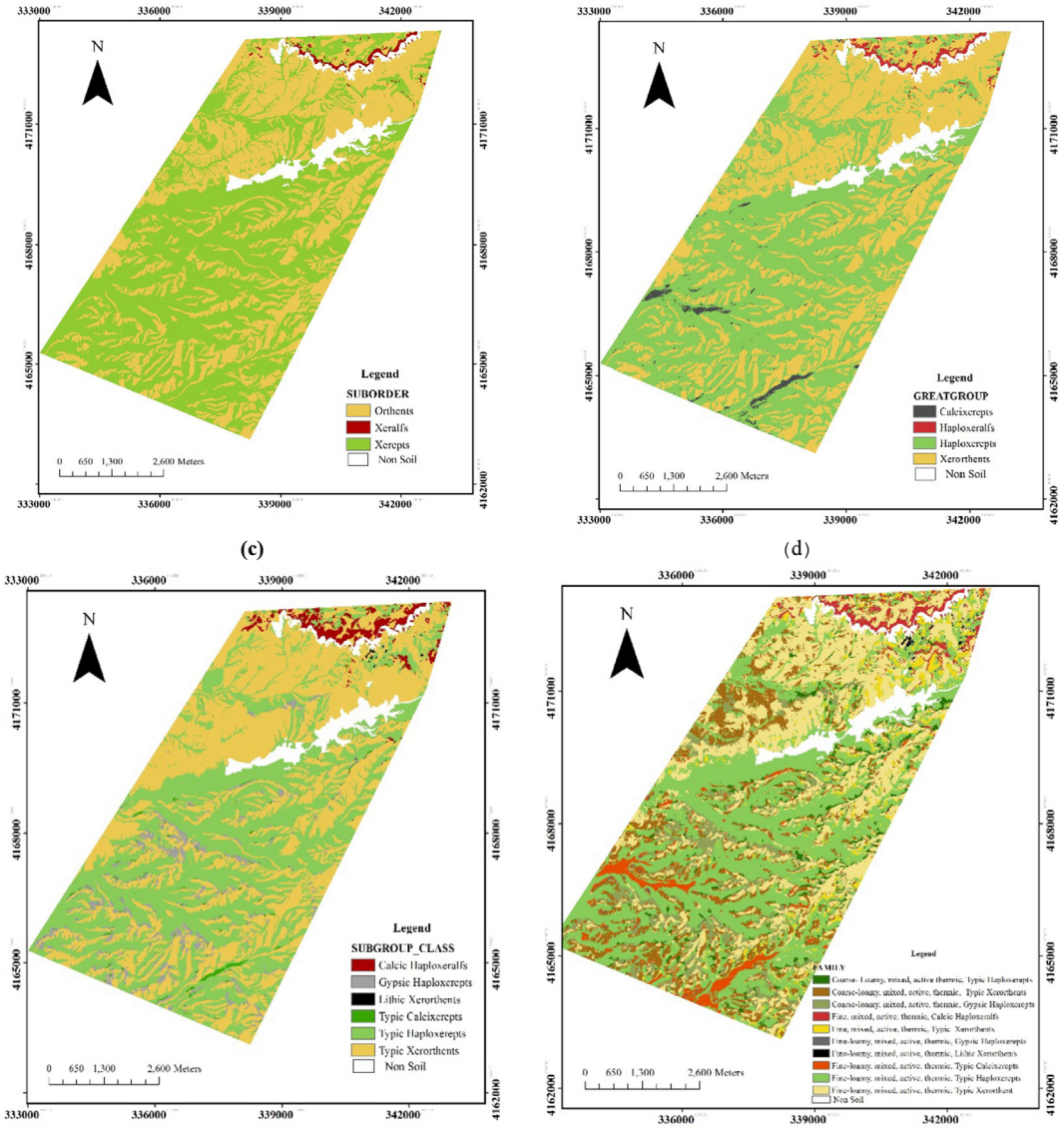

Fig. 4. Predicted soil map (a) suborder (b) great group (c) subgroup and (d) family levels.

hilly and mountainous areas. The choice of the optimal spatial resolution is still an open question that would require additional work, possibly with combinations of other methods like, e.g., photo interpretation (see Silva et al., 2019). It is expected that this ideal resolution will depend both on the topographic complexity of the landscape and on the environmental covariates to be used.

3.3.2. Covariates importance

Thirteen environmental covariates were considered at the comparison area, as presented in Fig. 8. Since some topographic attributes were constant over the area (e.g. curvature, profile curvature, and convergence), they were not used for the prediction.

According to both selection methods (Fig. 8), geomorphology, aspect, elevation, TPI, LS (excepted at suborder level) and SAVI (excepted at great group and subgroup levels) were identified as the most important environmental covariates for predicting the 5 m resolution soil map at the three lower taxonomic levels. Geomorphology, valley depth, elevation, aspect, LS (excepted at suborder level) and SAVI (excepted at great group and subgroup levels) were the most important ones for the 0.3 m resolution soil map at all taxonomic levels. Geomorphology and elevation have often been reported as potential predictors in DSM (Pahlavan Rad et al., 2014; Zeraatpisheh et al., 2017; Silva et al., 2019).

The aspect map is also an important environmental covariate that led to the correct identification of Haploxerepts and Xerorthents in the predicted map at 0.3 m resolution (Fig. 7b and 7c). These findings are confirmed by previous studies conducted by Kramm et al. (2017) and Maleki et al. (2018) in the Iranian loess plateau. As south-facing slopes are characterized by a limited vegetation cover (Fig. 7c) and high evaporation (to the opposite of north-facing slopes). SAVI is also directly related to these features (Maleki et al., 2018). This agrees with Pahlavan Rad et al. (2014), who identified SAVI as the most important covariate at all taxonomic levels when updating a soil map in Golestan province, Iran.

At the 0.3 m resolution, valley depth is also identified as an important covariate and is associated with the occurrence of a calcic horizon mapping unit (Fig. 7b), that typically occurs for low slopes and elevations and for high soil depths and vegetation cover areas. The results of Table 6 and Fig. 7 confirm this finding, as the Calcixerepts and Typic Calcixerepts classes were detected on valley landform where soil samples were available. Similarly, as reported by the Esfandiarpour-Boroujeni et al. (2020), valley depth is a covariate of major importance for predicting Calcic horizon in central Iran. These results show the potential of using topographic attributes derived from a high-resolution DEM when these attributes are intimately linked to the effective soil

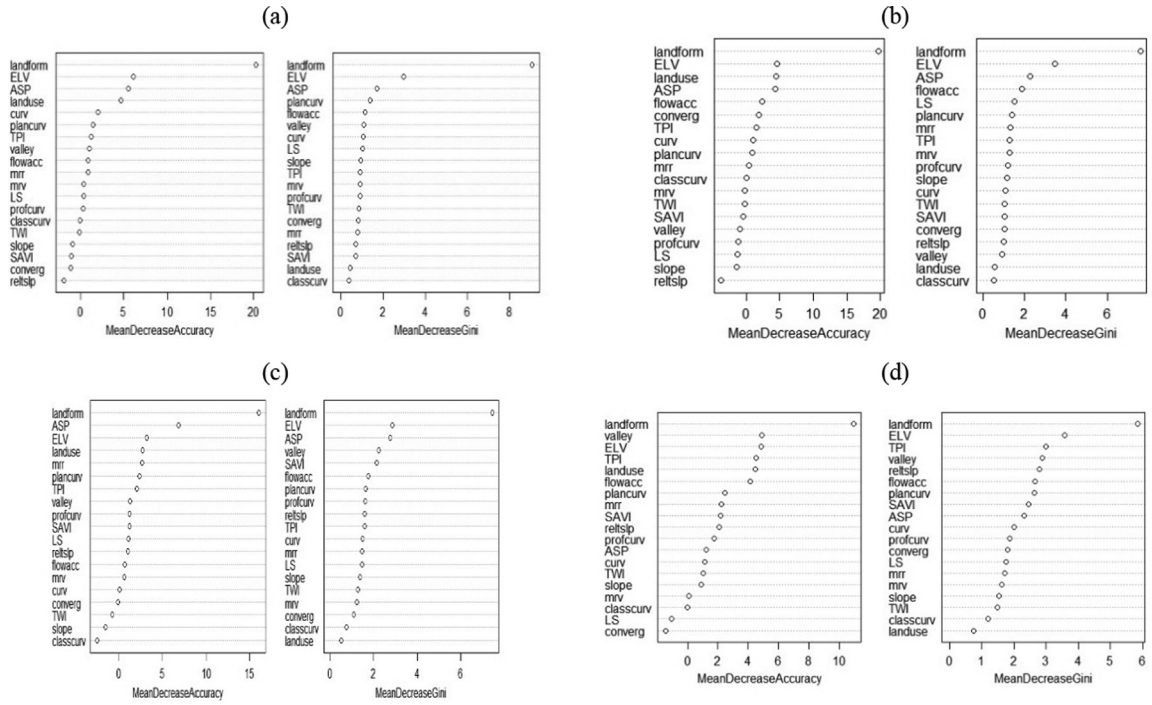

Fig. 5. Mean decrease of accuracy and mean decrease of Gini covariates importance for the study area (a) at suborder level, (b) at great group level, (c) at subgroup level and (d) at family level. Symbols for covariates are given in Table 2.

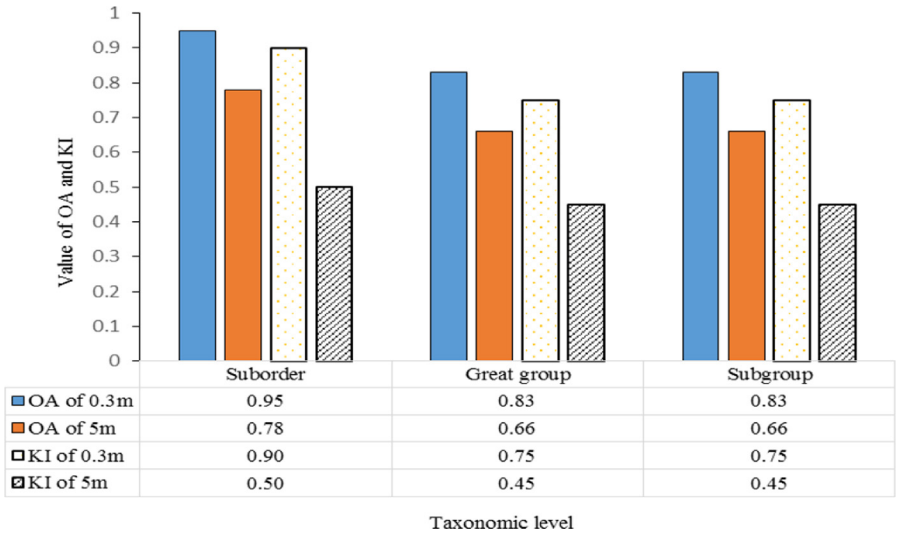

Fig. 6. Results for overall accuracy (OA) and Kappa index (KI) at different taxonomic levels using 0.3 m and 5 m spatial resolutions.

Table 6
Results for user's accuracy (UA), producer's accuracy (PA) and confusion idex (CI, i.e. uncertainty) at various soil taxonomic levels using DEMs with 0.3 m and 5 m spatial resolutions.

Level	Class	Frequency	CI		Area		UA (%)		PA (%)	
			0.3 m	5 m	0.3 m	5 m	0.3 m	5 m	0.3 m	5 m
Suborder	Xerepts	15	0.002–0.7	0.003–0.94	133	124	93.0	80.0	93.0	85.7
	Orthents	10			76	85	90.0	80.0	90.0	72.7
Great group	Haploxerepts	11	0.03–0.88	0–1	123	104	81.8	45.4	81.8	71.4
	Xerorthents	10			82	97	90.0	90.0	90.0	69.2
	Calcixerepts	4			4	8	75.0	75.0	60.0	50.0
Subgroup	Typic Haploxerepts	11	0.03–0.88	0–1	123	104	81.8	45.4	81.8	71.4
	Typic Xerorthents	10			82	97	90.0	90.0	90.0	69.2
	Typic Calcixerepts	4			4	8	75.0	75.0	60.0	50.0

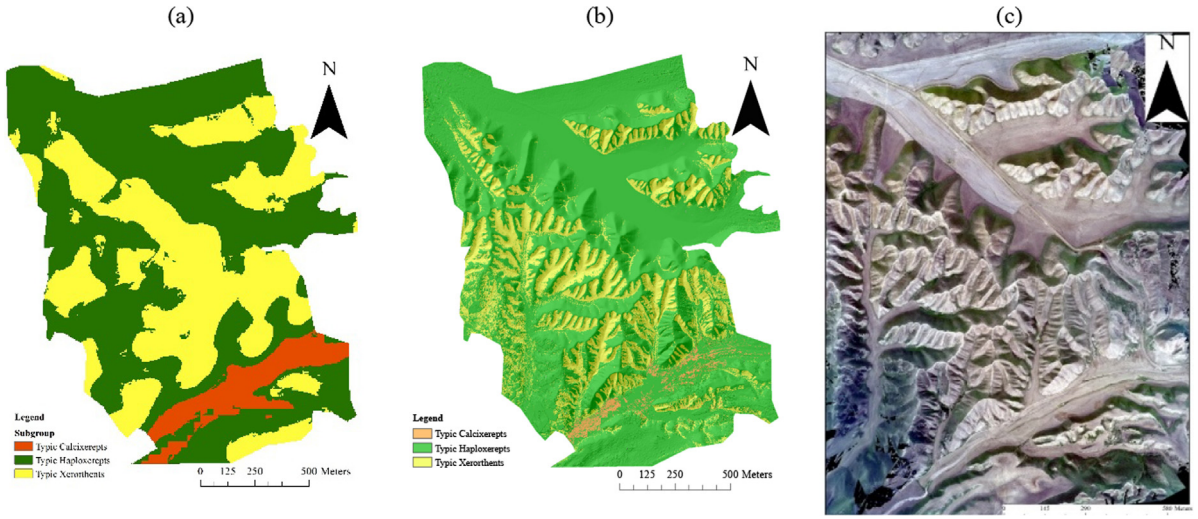

Fig. 7. Predicted soil maps at subgroup level (a) with DEM A and (b) with DEM B, along with (c) orthoimagery at the comparison area as obtained from UAV.

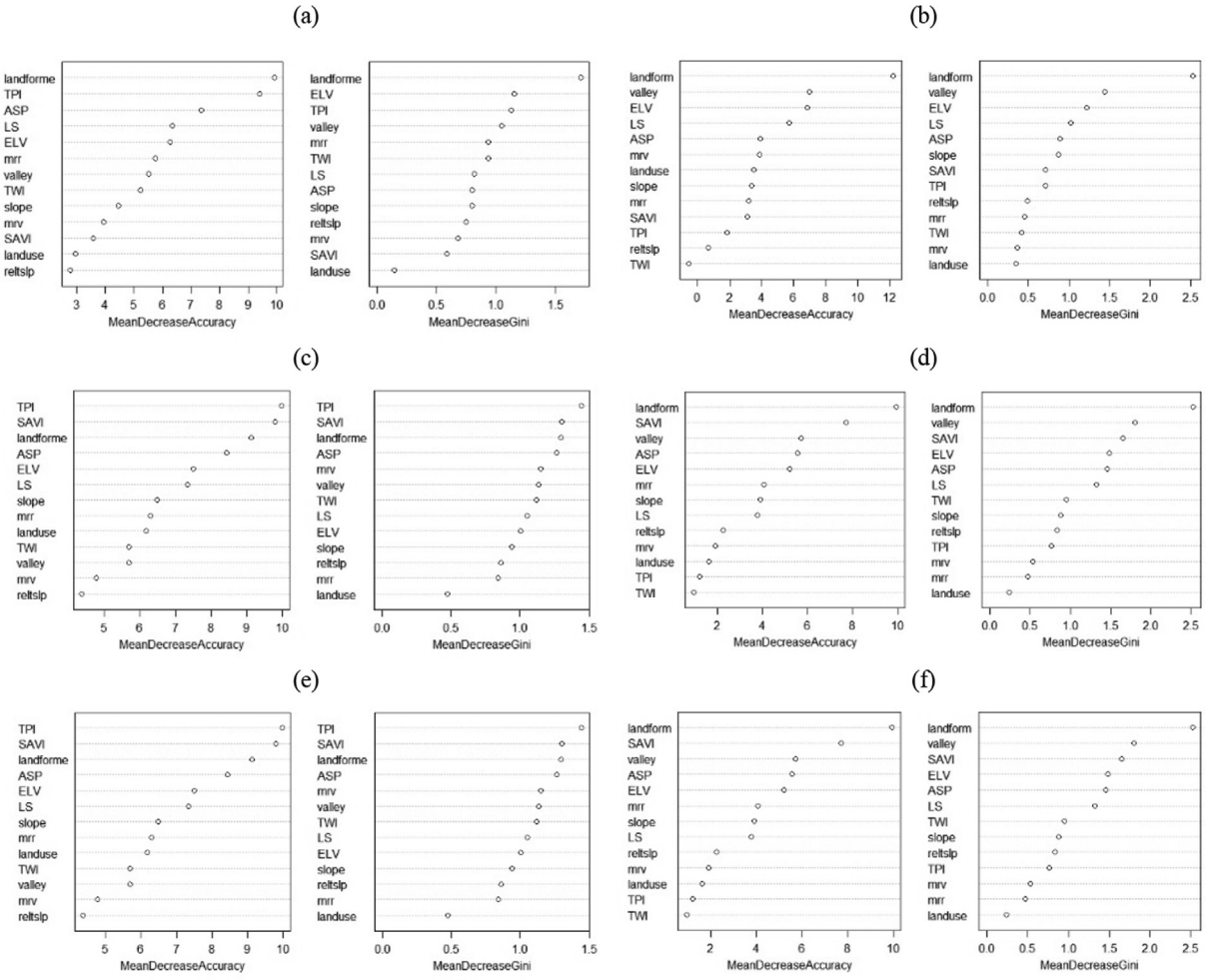

Fig. 8. Mean decrease of accuracy and mean decrease of Gini covariates importance for the comparison area. For the 5 m resolution, parts (a), (c) and (e) refers to the suborder level, great group level and subgroup level, respectively. For the 0.3 m resolution, parts (b), (d) and (f) refer to same levels, respectively. Symbols for covariates are given in Table 2.

forming factors. Whenever possible, our recommendation for preparing soil class maps at a larger scale is thus to use topographic attributes that are extracted from high-resolution DEMs, possibly using UAV techniques.

4. Conclusions

The effect of the accuracy of topographic attributes for improving DSM prediction were investigated in a semiarid region of Iran using two datasets of environmental covariates and accounting for two spatial

resolutions of these covariates. More specifically, we investigated how high-resolution environmental covariates (geomorphology maps and DEM-derived topographic attributes using an UAV technique) could help predict soil maps at various taxonomic levels using limited soil data. Based on covariates importance assessment, the geomorphology map and some topographic attributes were identified as the most important ones at all taxonomic levels. Using topographic attributes at a 0.3 m spatial resolution improved overall accuracy and Kappa index, leading to predicted soil maps that are also in agreement with orthophotos over the study area. In addition, the results demonstrated that the model accuracy is not the only factor to be accounted for when interpreting the quality of a map, as uncertainty is important as well. However, using higher resolution attributes does not automatically lead to better results, as the proper identification of pedogenic properties and soil forming factors influenced soil development is of major importance. It can be concluded that a combination of sound DSM methods, high-precision environmental data and expert knowledge could lead to a reduced need for soil samples. This is particularly beneficial for mapping large areas in areas that are facing a shortage of soil data, as it is the case in Iran.

Declaration of Competing Interest

The authors declared that there is no conflict of interest.

Acknowledgements

The authors gratefully acknowledge the two anonymous reviewers for their constructive comments that greatly helped improve this manuscript.

References

Abbaszadeh Afshar, F., Ayoubi, S.h., Jafari, A., 2018. The extrapolation of soil great groups using multinomial logistic regression at regional scale in arid regions of Iran. Geoderma 315, 36–48. https://doi.org/10.1016/j.geoderma.2017.11.030.

Arrouays, D., McKenzie, N., Hempel, J., de Forges, A., McBratney, A.B., 2014. GlobalSoilMap: Basis of the Global Spatial Soil Information System. CRC Press.

Arrouays, D., McBratney, A.B., Bouma, J., Libohova, Z., Richer-de-Forges, A.C., Morgan, L.S.C., Roudier, P., Poggio, L., Leatitia Mulder, V., 2020. Impressions of digital soil maps: The good, the not so good, and making them ever better. Geoderma Reg. 20, e00255. https://doi.org/10.1016/j.geodrs.2020.e00255.

Bagheri Bodaghabadi, M., Martinez-Casasnovas, J.A., Esfandiarpoor Borujeni, I., Salehi, M.H., Mohammadi, J., Toomanian, N., 2016. Database extension for digital soil mapping using artificial neural networks. Arab. J. Geosci. 9, 701. https://doi.org/10.1007/s12517-016-2732-z.

Barneveld, R., Seeger, M., Maalen-Johansen, I., 2013. Assessment of terrestrial laser scanning technology for obtaining high-resolution DEMs of soils. Earth Surf. Processes Landforms. 38, 90–94. https://doi.org/10.1002/esp.3344.

Behrens, T., Förster, H., Scholten, T., Steinrücken, U., Spies, E.D., Goldschmitt, M., 2005. Digital soil mapping using artificial neural networks. J. Plant Nutr. Soil Sci. 168 (1), 21–33. https://doi.org/10.1002/jpln.200421414.

Bouma, J., 1997. Soil environmental quality: A European perspective. J. Environ. Qual. 26, 26–31. https://doi.org/10.2134/jeq1997.00472425002600010005x.

Breiman, L., 2001. Random forests. Mach. Learn. 45 (1), 5–32. https://doi.org/10.1023/A:1010933404324.

Breiman, L., Cutler, A., 2004. Random Forests homepage. Retrieved April 23rd.

Brungard, C.W., 2009. Alternative sampling and analysis methods for digital soil mapping in Southwestern Utah. Thesis for Master of Science, Utah State University, USA, 284p.

Brungard, C.W., Boettinger, J.L., Duniway, M.C., Wills, S.A., Edwards Jr., T.C., 2015. Machine learning for predicting soil classes in three semi-arid landscapes. Geoderma 239–240, 68–83. https://doi.org/10.1016/j.geoderma.2014.09.019.

Brus, D.J., Kempen, B., Heuvelink, G.B.M., 2011. Sampling for validation of digital soil maps. Eur. J. Soil Sci. 62, 394–407. https://doi.org/10.1111/j.1365-2389.2011.01364.x.

Camera, C., Zomeni, Z., Noller, J.S., Zissimos, A.M., Christoforou, I.C., Bruggeman, A., 2017. A high resolution map of soil types and physical properties for Cyprus: A digital soil mapping optimization. Geoderma 285, 35–49. https://doi.org/10.1016/j.geoderma.2016.09.019.

Cavazzi, S., Corstanje, R., Mayr, Th., Hannam, J., Fealy, R., 2013. Are fine resolution digital elevation models always the best choice in digital soil mapping? Geoderma 195–196, 111–121. https://doi.org/10.1016/j.geoderma.2012.11.020.

Dà-Jiāng Innovations Science and Technology Co (DJI), 2016. Phantom 3 Professional User Manual v1.8; DJI: Shenzhen, China.

Dobos, E., Montanarella, L., Nègre, T., Micheli, E., 2001. A regional scale soil mapping approach using integrated AVHRR and DEM data. Int. J. Appl. Earth Obs. Geoinf. 3 (1), 30–42. https://doi.org/10.1016/S0303-2434(01)85019-4.

Emadi, M., Baghernejad, M., 2014. Comparison of spatial interpolation techniques for mapping soil pH and salinity in agricultural coastal areas, northern Iran. Arch. Agron. Soil Sci. 60 (9), 1315–1327. https://doi.org/10.1080/03650340.2014.880837.

Esfandiarpour-Boroujeni, I., Shahini-Shamsabadi, M., Shirani, H., Mosleh, Z., Bagheri-Bodaghabadi, M., Salehi, M.H., 2020. Assessment of different digital soil mapping methods for prediction of soil classes in the Shahrekord plain. Central Iran. Catena 193, 104648. https://doi.org/10.1016/j.catena.2020.104648.

Fabris, M., Pesci, A., 2005. Automated DEM extraction in digital aerial photogrammetry: precision and validation for mass movement monitoring. Ann. Geophys. 48, 973–988. https://doi.org/10.4401/ag-3247.

Feiznia, S., Ghauomian, J., Khadjeh, M., 2005. The study of the effect of physical, chemical, and climate factors on surface erosion sediment yield of loess soils (Case study in Golestan province). Pajouhesh & Sazandegi 66, 14–24 (In Persian with English abstract).

Gallant, J.C., Dowling, T.I., 2003. A multi resolution index of valley bottom flatness for mapping depositional areas. Water Resour. Res. 39, 1347–1360.

Grimm, R., Behrens, T., Märker, M., Elsenbeer, H., 2008. Soil organic carbon concentrations and stocks on Barro Colorado Island—digital soil mapping using RandomForests analysis. Geoderma 146 (1), 102–113. https://doi.org/10.1016/j.geoderma.2008.05.008.

Hengl, T., 2006. Finding the right pixel size. Comput. Geosci. 32 (9), 1283–1298. https://doi.org/10.1016/j.cageo.2005.11.008.

Höhle, J., 2009. Dem generation using a digital large-format frame camera. Photogramm. Eng. Remote. Sens. 75, 87–93. https://doi.org/10.14358/PERS.75.1.87.

Hosseinalizadeh, M., Kariminejad, N., Rahmati, O., Keesstra, S., Alinejad, M., Mohammadian Behbahani, A., 2019a. How can statistical and artificial intelligence approaches predict piping erosion susceptibility? Sci. Total Environ. 646, 1554–1566. https://doi.org/10.1016/j.scitotenv.2018.07.396.

Hosseinalizadeh, M., Kariminejad, N., Chen, W., Pourghasemi, H.R., Alinejad, M., Mohammadian Behbahani, A., Tiefenbacher, J.P., 2019b. Spatial modelling of gully headcuts using UAV data and four best-first decision classifier ensembles (BFTree, Bag-BFTree, RS-BFTree, and RF-BFTree). Geomorphology 329, 184–193. https://doi.org/10.1016/j.geomorph.2019.01.006.

Hu, S.H., Qiu, H., Wang, Xingang X., Gao, Y., Wang, N., Wu, J., Yang, D., Cao, M., 2018. Acquiring high-resolution topography and performing spatial analysis of loess landslides by using low-cost UAVs. Landslides 15, 593–612. https://doi.org/10.1007/s10346-017-0922-8.

Huete, A.R., 1988. A soil adjusted vegetation index (SAVI). Remote Sens. Environ. 25, 295–309. https://doi.org/10.1016/0034-4257(88)90106-X.

Jafari, A., Ayoubi, S., Khademi, H., Finke, P.A., Toomanian, N., 2013. Selection of a taxonomic level for soil mapping using diversity and map purity indices: A case study from an Iranian arid region. Geomorphology 12. https://doi.org/10.1016/j.geomorph.2013.06.010.

Keesstra, S.D., Bouma, J., Wallinga, J., Tittonell, P., Smith, P., Cerda, A., Montanarella, L., Quinton, J.N., Pachepsky, Y., van der Putten, W.H., Bardgett, R.D., 2016. The significance of soils and soil science towards realization of the United Nations sustainable development goals. Soil 2 (2), 111–128. https://doi.org/10.5194/soil-2-111-2016.

Khaledian, Y., Miller, B.A., 2019. Selecting appropriate machine learning methods for digital soil mapping. Math. Model Appl. https://doi.org/10.1016/j.apm.2019.12.016.

Khormali, F., Kehl, M., 2011. Micromorphology and development of loess-derived surface and buried soils along a precipitation gradient in Northern Iran. Quat. Int. 234, 109–123. https://doi.org/10.1016/j.quaint.2010.10.022.

Kempen, B., Brus, D.J., Heuvelink, G.B.M., Stoorvogel, J.J., 2009. Updating the 1:50,000 Dutch soil map using legacy soil data: a multinomial logistic regression approach. Geoderma 151, 311–326. https://doi.org/10.1016/j.geoderma.2009.04.023.

Kramm, T., Hoffmeister, D., Curdt, C., Maleki, S., Khormali, F., Kehl, M., 2017. Accuracy assessment of landform classification approaches on different spatial scales for the Iranian loess plateau. ISPRS Int. J. Geo-Inf. 6 (366), 418 1–418 22. https://doi.org/10.3390/ijgi6110366.

Kung, O., Strecha, C., Beyeler, A., Zufferey, J.C., Floreano, D., Fua, P., Gervaix, F., 2011. The accuracy of automatic photogrammetric techniques on ultra-light UAV imagery. Int. Arch. Photogramm. Remote. Sens. Spat. Inf. Sci. XXXVIII, 1–7. https://doi.org/10.5194/isprsarchives-XXXVIII-1-C22-125-2011.

Lagacherie, P.H., Arrouays, D., Bourennane, H., Gomez, C., Martin, M., Saby, N.P.A., 2019. How far can the uncertainty on a Digital Soil Map be known?: A numerical experiment using pseudo values of clay content obtained from Vis-SWIR hyperspectral imagery. Geoderma. https://doi.org/10.1016/j.geoderma.2018.08.024. (Article in press).

Lacoste, M., Minasny, B., McBratney, A., Michot, D., Viaud, V., Walter, C., 2014. High resolution 3D mapping of soil organic carbon in a heterogeneous agricultural landscape. Geoderma 213, 296–311. https://doi.org/10.1016/j.geoderma.2013.07.002.

Laliberte, A., Herrick, J., Rango, A., Winters, C., 2010. Acquisition, orthorectification, and object-based classification of unmanned aerial vehicle (UAV) imagery for rangeland monitoring. Photogramm. Eng. Remote. Sens. 76, 661–672.

Liaw, A., Wiener, M., 2002. Classification and regression by random forest. R New 2 (3), 18–22.

Liu, Y., Zheng, X., Ai, G., Zhang, Y., Zuo, Y., 2018. Generating a high-precision true digital orthophoto map based on UAV images. Int. J. Geo-Inf. 7, 333. https://doi.org/10.3390/ijgi7090333.

Machado, D.F.T., de Menezes, M.D., Silva, S.H.G., Nilton Curi, C., 2019. Transferability, accuracy, and uncertainty assessment of different knowledge-based approaches for soil types mapping. Catena 182, 104134. https://doi.org/10.1016/j.catena.2019.

104134.
MathWorks, 2009. Matlab. The Math Works. Inc., Natick, MA.
Maleki, S., Khormali, F., Bagheri Bodaghabadi, M., Mohammadi, J., Hoffmeister, D., Kehl, M., 2018. Role of geomorphic surface on the above-ground biomass and soil organic carbon storage in a semi-arid region of Iranian loess plateau. Quat. Int. https://doi.org/10.1016/j.quaint.2018.11.001.
Marchetti, A., Piccini, C., Santucci, S., Chiuchiarelli, I., Francaviglia, R., 2011. Simulation of soil types in Teramo province (Central Italy) with terrain parameters and remote sensing data. Catena 85, 267–273. https://doi.org/10.1016/j.catena.2011.01.012.
McBratney, A.B., Mendonc Santos, M.L., Minasny, B., 2003. On digital soil mapping. Geoderma 117, 3–52. https://doi.org/10.1016/S0016-7061(03)00223-4.
Mirakzehi, K.h., Pahlavan Rad, M.R., Shahriari, A., Bameri, A., 2018. Digital soil mapping of deltaic soils: A case of study from Hirmand (Helmand) river delta. Geoderma 313, 233–240. https://doi.org/10.1016/j.geoderma.2017.10.048.
Minasny, B., McBratney, A.B., 2006. A conditioned Latin hypercube method for sampling in the presence of ancillary information. Comput. Geosci. 32, 1378–1388. https://doi.org/10.1016/j.cageo.2005.12.009.
Minasny, B., Bishop, T.F.A., 2008. Analysing uncertainty. In: McKenzie, N.J., Grundy, M.J., Webster, R., Ringrose-Voase, A.J. (Eds.), Guidelines for Surveying Soil and Land Resources, second ed. CSIRO Publishing, Collingwood, pp. 383–394.
Mohammadi, J., Shataee, Sh., Namiranian, M., Næsset, E., 2017. Modeling biophysical properties of broad-leaved stands in the hyrcanian forests of Iran using fused airborne laser scanner data and ultraCam-D images. Int. J. Appl Earth Obs. Geoinform. 61, 32–45. https://doi.org/10.1016/j.jag.2017.05.003.
Mosleh, Z., Salehi, M.H., Jafari, A., Borujeni, I.E., Mehnatkesh, A., 2016. The effectiveness of digital soil mapping to predict soil properties over low-relief areas. Environ. Monit. Assess. 188, 1–13. https://doi.org/10.1007/s10661-016-5204-8.
Myles, A.J., Feudale, R.N., Liu, Y., Woody, N.A., Brown, S.D., 2004. An introduction to decision tree modeling. J. Chemom. 18 (6), 275–285.
Mulder, V.L., de Bruin, S., Schaepman, M.E., Mayr, T.R., 2011. The use of remote sensing in soil and terrain mapping – a review. Geoderma 162 (1), 1–19. https://doi.org/10.1016/j.geoderma.2010.12.018.
Mukherjee, S., Joshi, P.K., Mukherjee, S., Ghosh, A., Garg, R.D., Mukhopadhyay, A., 2013. Evaluation of vertical accuracy of open source digital elevation model (DEM). Int. J. Appl. Earth Obs. Geoinf. 21, 205–217. https://doi.org/10.1016/j.jag.2012.09.004.
Olaya, V.F., 2004. A Gentle Introduction to Saga GIS. The SAGA User Group eV, Gottingen, Germany, pp. 208.
Pain, C.F., 2005. Size does matter: relationships between image pixel size and landscape process scales. MODSIM 2005 International Congress on Modeling and Simulation, pp. 1430–1436.
Pahlavan Rad, M.R., Toomanian, N., Khormali, F., Brungard, C.W., Komaki, C.B., Bogaert, P., 2014. Updating soil survey maps using random forest and conditioned Latin hypercube sampling in the loess derived soils of northern Iran. Geoderma 232–234, 97–106. https://doi.org/10.1016/j.geoderma.2014.04.036.
Peters, J., De Baets, B., Verhoest, N.E., Samson, R., Degroeve, S., De Becker, P., Huybrechts, W., 2007. Random forests as a tool for ecohydrological distribution modelling. Ecol. Model. 207 (2), 304–318. http://hdl.handle.net/1854/LU-381902.
Rasaei, Z., Bogaert, P., 2019. Bayesian data fusion for combining maps of predicted soil classes: A case study using legacy soil profiles and DEM covariates in Iran. Catena 182, 104–138. https://doi.org/10.1016/j.catena.2019.104138.
R Development Core Team, 2017. R: A language and environment for statistical computing. R Foundation for Statistical Computing, Vienna, Austria. Retrieved from http://www.R-project.org.
Rossiter, D.G., 2000. Methodology for soil resource inventories, 2nd revised version, soil science devision, international institute for aerospace survey and earth science (ITC), 132 pp.
RStudio, 2017. RStudio: Integrated Development Environment for R, Boston, MA. http://www.r-studio.com.
Silva, B.P.E.C., Silva, M.L.N., Avalos, F.A.P.O., Menezes, M.D., Nilton Curi, N., 2019. Digital soil mapping including additional point sampling in Posses ecosystem services pilot watershed, southeastern Brazil. Sci. Rep. 9, 13763. https://doi.org/10.1038/s41598-019-50376-w.
Sreenivas, K., Dadhwal, V.K., Kumar, S., Harsha, G.S., Mitran, T., Sujatha, G., Janaki Rama Suresh, G., Fyzee, M.A., Ravisankar, T., 2016. Digital mapping of soil organic and inorganic carbon status in India. Geoderma 269, 160–173. https://doi.org/10.1016/j.geoderma.2016.02.002.
Stoorvogel, J.J., Kempen, B., Heuvelink, G.B.M., de Bruin, S., 2009. Implementation and evaluation of existing knowledge for digital soil mapping in Senegal. Geoderma 149, 161–170. https://doi.org/10.1016/j.geoderma.2008.11.039.
Stoorvogel, J.J., Kooistra, L., Bouma, J., 2015. Managing soil variability at different spatial scales as a basis for precision agriculture. In: Lal, R., Stewart, B.A. (Eds.), Soil-Specific Farming: Precision Agriculture (Advances in Soil Science). CRC Press, pp. 37–72. https://doi.org/10.1201/b18759-3.
Soil Survey Staff, 2014. Keys to Soil Taxonomy (12th ED), U.S. Department of Agriculture, Natural Resources Conservation Service, pp. 372.
Taghizadeh-Mehrjardi, R., Minasny, B., Sarmadianc, F., Malone, B.P., 2014. Digital mapping of soil salinity in Ardakan region, central Iran. Geoderma 213, 15–28. https://doi.org/10.1016/j.geoderma.2013.07.020.
Taghizadeh-Mehrjardi, R., Nabiollahi, K., Kerry, R., 2016. Digital mapping of soil organic carbon at multiple depths using different data mining techniques in Baneh region, Iran. Geoderma 266, 98–110. https://doi.org/10.1016/j.geoderma.2015.12.003.
Taheri, M., Khormali, F., Wang, X., Amini, A., Wei, H.T., Kehl, M., Frechen, M., Chen, F.H., 2016. Micromorphology of the Lower Pleistocene Loess in the Iranian Loess Plateau and its paleoclimatic implications. Quat. Int. 429, 31–40. https://doi.org/10.1016/j.quaint.2016.01.063.
Teng, H., Viscarra Rossel, R.A., Shi, Z.H., Behrens, T.H., 2018. Updating a national soil classification with spectroscopic predictions and digital soil mapping. Catena 164, 125–134. https://doi.org/10.1016/j.catena.2018.01.015.
Toomanian, N., Jalalian, A., Khademi, H., Karimian Eghbal, M., Papritz, A., 2006. Pedodiversity and pedogenesis in Zayandeh-rud Valley, Central Iran. Geomorphology 81, 376–393. https://doi.org/10.1016/j.geomorph.2006.04.016.
Wang, Sh., Jin, X., Adhikari, K., Li, W., Yu, M., Bian, Zh., Wang, Q., 2018. Mapping total soil nitrogen from a site in northeastern China. Catena 166, 134–146. https://doi.org/10.1016/j.catena.2018.03.023.
Weiss, A.D., 2001. Topographic position and landforms analysis, in Proceedings of the ESRI User Conference, 9-13 July, San Diego, CA, USA.
Wilson, J.P., Gallant, J.C., 2000. Terrain analysis. Wiley & Sons, New York.
Vega, F., Ramírez, F., Siaz, M., Rosua, F., 2015. Multi-temporal imaging using an unmanned aerial vehicle for monitoring a sunflower crop. Biosyst. Eng. 132, 19–27. https://doi.org/10.1016/j.biosystemseng.2015.01.008.
Viloria, J.A., Viloria-Botello, A., Pineda, M.C., Valera, A., 2016. Digital modelling of landscape and soil in a mountainous region: a neuro-fuzzy approach. Geomorphology 253, 199–207. https://doi.org/10.1016/j.geomorph.2015.10.007.
Yiming, A., Lin, Y., A-Xing, Z., Chengzhi, Q., JingJing, S., 2017. Identification of representative samples from existing samples for digital soil mapping. Geoderma 311, 109–119. https://doi.org/10.1016/j.geoderma.2017.03.014.
Zeraatpisheh, M., Ayoubi, Sh., Jafari, A., Finke, P., 2017. Comparing the efficiency of digital and conventional soil mapping to predict soil types in a semi-arid region in Iran. Geomorphology 285, 186–204. https://doi.org/10.1016/j.geomorph.2017.02.015.
Zeraatpisheh, M., Jafari, A., Bodaghabadi Bodaghabadi, M., Ayoubi, S., Taghizadeh-Mehrjardi, R., Toomanian, N., Kerry, R., Xu, M., 2020. Conventional and digital soil mapping in Iran: Past, present, and future. Catena 188, 104424. https://doi.org/10.1016/j.catena.2019.104424.
Zinck, J.A., 1989. Physiography and soils. Lecture Notes for Soil Students. Soil Science Division. Soil Survey Courses Subject Matter: K6 ITC, Enschede, the Netherlands.
Zhao, Zh., Yang, Q., Sun, D., Ding, X., Meng, F.R., 2020. Extended model prediction of high-resolution soil organic matter over a large area using limited number of field samples. Comput. Electron. Agr. 169, 105172. https://doi.org/10.1016/j.compag.2019.105172.
Zhi, J., Zhang, G., Yang, F., Yang, R., Liu, F., Song, X., Zhao, Y., Li, D., 2017. Predicting mattic epipedons in the northeastern Qinghai-Tibetan plateau using random forest. Geoderma Regional 10, 1–10. https://doi.org/10.1016/j.geodrs.2017.02.001.
Zhu, A., Yang, L., Li, B., Qin, C., English, E., Burt, J.E., Zhou, C., 2008. Purposive sampling for digital soil mapping for areas with limited data. In: Hartemink, A.E., McBratney, A.B., Mendonca Santos, M.L. (Eds.), Digital Soil Mapping with Limited Data. Springer-Verlag Inc., New York, pp. 233–245. https://doi.org/10.1007/978-1-4020-8592-5_20.